Increasing the Energy-Efficiency of Induction Machines by the Use of Grain-Oriented Magnetic Materials and Die-Casting Copper Squirrel Cage in the Rotor

Vincent Mallard, Guillaume Parent, C. Demian, Jean-François Brudny, Aurélien Delamotte

Increasing the Energy-Efficiency of Induction Machines by the Employment of Grain-Oriented Magnetic Materials and Die-Casting Copper Squirrel Cage in the Rotor

Vincent Mallard*†, Guillaume Parent*, Cristian Demian*, Jean-François Brudny*, Aurélien Delamotte†
*Univ. Artois, EA 4025, Laboratoire Systèmes Électrotechniques et Environnement (LSEE), F-62400 Béthune, France
†FAVI SA, F-80490 Hallencourt, France

***Abstract*— This paper deals with the results of an experimental prototype for a new magnetic structure, which is based on a non segmented lamination with grain oriented electrical steel sheets in order to reduce core losses. This structure was applied to a rotor with die casting copper squirrel cage.**
***Topic*—Induction machine, magnetic cores, magnetic losses, die casting, copper squirrel-cage.**

I. Introduction

Nowadays, increasing the efficiency of electrical motors has become a priority in order to reduce electricity consumption and CO_2 emissions. This is why an International Standard [1], dated 2011, specifies a minimum efficiency for electrical motors. A lot of studies on the subject can be found in the literature. The most common technique used by machine manufacturers is the core-stack length approach [2,3] which simply consists in increasing the stack length. However this concept is limited, particularly when the machines are already IE3 or IE4 [4]. Another approach consists in replacing aluminium by copper in the squirrel cage [5]–[7]. Using that kind of rotor squirrel cage can significantly reduce rotor Joule losses compared to an aluminium one and leads to a reduction of the motors volume while keeping the same performance. Another method is to use grain-oriented (GO) electrical steel sheets in place of non-oriented (NO) ones. This technology is particularly suited for segmented laminations, as in the case of permanent magnet synchronous machines [8] and switched reluctance machines [9], but can also be applied to non-segmented induction machines stators [10].

Works presented in this paper deal with the study of an induction machine composed of a copper squirrel cage and a rotor core made of non-segmented laminations. In the first part, the approach consists in investigating the impact of a non-segmented GO magnetic circuit with a simple experimental structure [11]. The latter, which can be qualified as ”static machine”, has the same behaviour as a transformer under rotating field conditions and allows to compare cores made of different electrical steel sheets grade and thickness. In the second part, the conclusions made on static machines are validated by a comparison between two induction machines, one with a rotor made of NO laminations, the other one with a rotor made of GO laminations.

II. Experimentation with Static Machine

A. Static Machine

The first part of the study presented in this paper is performed on static machines (Fig. 1a), whose behaviour is similar to transformers under rotating field conditions, but correspond to actual four-pole induction machines design without rotor slots. Moreover, three small joints make the rotor fastened to the stator as well as they ensure the air gap to be uniform. They are designed such that their cores require few magnetic field to be saturated. As for the electrical circuit, it is composed of two four-pole three-phase star-connected windings. The first one, composed of five turns, is used to feed the machine whereas the second one, composed of one turn, is devoted to the electromotive force measurement. Such a device allows to test different magnetic circuit assembly configurations, which would hardly be possible with actual inductions machines due to construction time and cost.

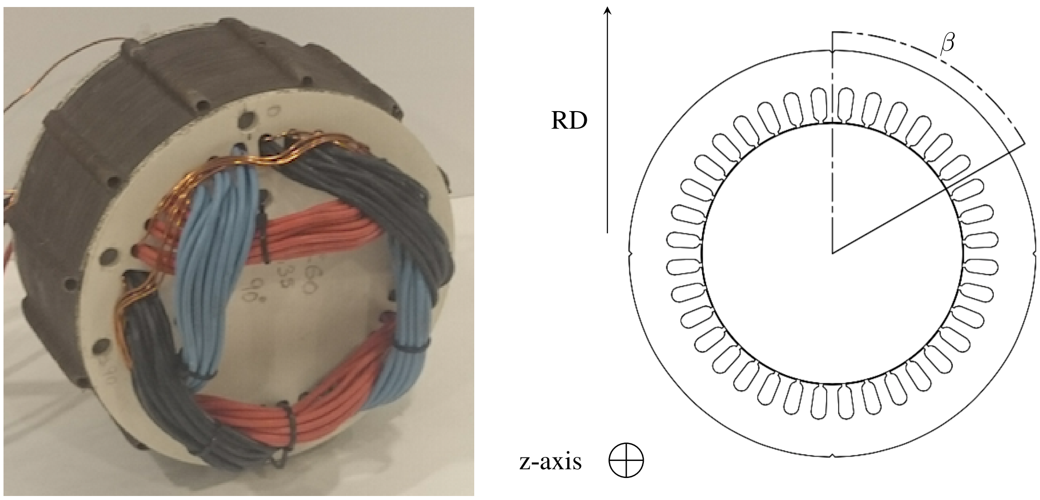

(a) (b)

Fig. 1. Static machine

B. Shifted Magnetic Circuit Method

GO electrical steel present a very high anisotropic behaviour. It has an easy magnetization direction at [001] 0° of crystallographic plane, corresponding to the Rolling Direction (RD), and a hard one at [111] 55°. Hence, in order to use GO non-segmented laminations under rotating field conditions, it is obvious that a shifted stack is required in order for the flux to be able to take advantage of each lamination RD [12]. The magnetic core is then obtained by shifting each lamination to the other by an angle β referring to the RD as illustrated in Fig. 1b. A previous work [11] showed that the optimal value of β in terms of energy efficiency is found at 90°.

C. Core losses measurement

As stated in section II-A, the static machine rotor can not enter into rotation, contrary to an actual induction machine. Two conclusions can be deduced from that: static machines can be considered as transformers and their rotor and stator magnetic fluxes share the same frequency. This is why the equivalent single-phase scheme presented in Fig. 2 can be used for its modeling, where R_p represents the primary winding copper losses, X_p is the primary winding leakage inductance, X_μ represents the reactive power required to magnetize the machine.

R_s and X_s represent the secondary Joule losses and the flux leakage inductance respectively. The electrical variables such as $\underline{V}_\mathrm{p}$ is the primary voltage, $\underline{I}_\mathrm{p}$ is the primary current, $\underline{E}_\mathrm{p}$ represents the electromotive force seen from the primary, $\underline{E}_\mathrm{s}$ represents the electromotive force seen from the secondary and $\underline{V}_\mathrm{s}$ is the secondary voltage. The last parameters m s the turn ratio.

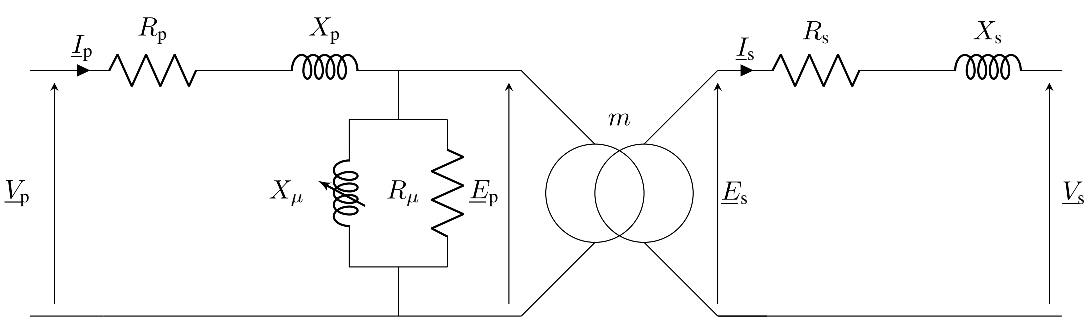

Fig. 2. Equivalent single-phase scheme

TABLE I
STATIC MACHINE CONFIGURATIONS

Configurations	**Materials**
1	NO50
2	NO35
3	CGO35
4	HGO35

D. Measurements

As stated in section II-C, the rotor and the stator magnetic cores share the same magnetic flux frequency. That is why, the rotor and stator core losses can be grouped into one component. Hence, in Fig. 2, R_μ represents the global core losses. In order to determine R_μ, a sinusoidal voltage is applied to the primary winding ($\underline{V}_\text{p}$). The power meter is used to measure the stator current $\underline{I}_\text{p}$ and the secondary voltage $\underline{V}_\text{s}$. In this context, our experiment can be assimilated to a no-load test. As a consequence, there is no current in the secondary winding, which leads to $\underline{V}_\text{s} = \underline{E}_\text{s}$. According to the section II-A, the primary and secondary windings are implemented in two identical sections with a different number of turns. Hence, the electromotive force in the primary winding can be expressed by (1) because the phase shift between $\underline{E}_\text{s}$ and $\underline{E}_\text{p}$ does not exist in this case. Therefore, the core losses can be written in (2), where φ is the phase shift between the stator current $\underline{I}_\text{p}$ and the electromotive force $\underline{E}_\text{s}$. Hence, R_μ can be defined by (3). The main advantage of this measurement procedure is that the primary Joule losses and the primary leakage inductance are not to be taken into account.

$$E_\text{p} = \frac{E_\text{s}}{m} \tag{1}$$

$$P_\mu = 3mE_\text{s}I_\text{p}\cos\varphi \tag{2}$$

$$R_\mu = \frac{3E_\text{p}^2}{P_\mu} \tag{3}$$

The air-gap induction $\hat{b_{ag}}$ is a key parameter in an electrical machine design. That is why, the result are expressed as at different levels of $\hat{b_{ag}}$. Hence, $\hat{b_{ag}}$ can be expressed by(4) where n_a represents the number of turn of the secondary winding, k_a is the winding coefficient of the secondary winding, R is the rotor radius and l is the active length.

$$\hat{b_{ag}} = \frac{\sqrt{2}E_\text{s}}{2n_\text{a}k_\text{a}Rl\omega} \tag{4}$$

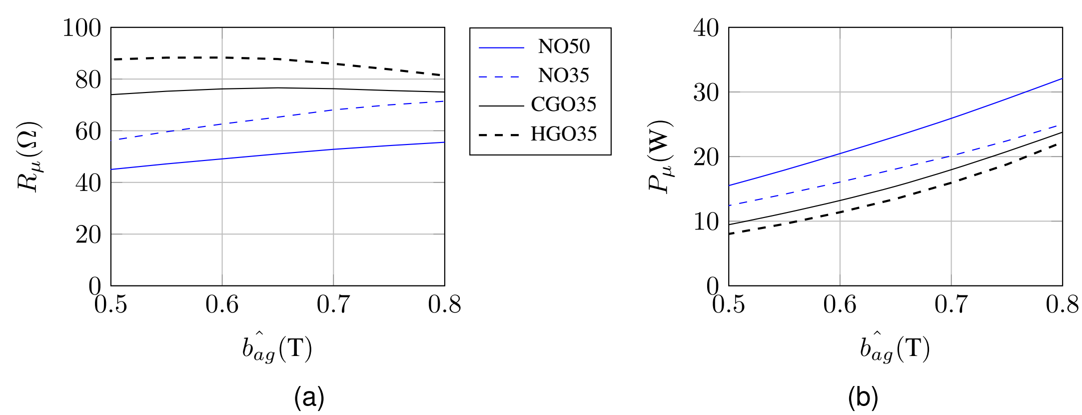

Fig. 3. (a) R_μ at different $\hat{b_\text{ag}}$ levels, (b) P_μ at different $\hat{b_\text{ag}}$ levels.

E. Results

The different grades used to make these static machines are shown in Table. I. Two kind of GO materials, conventional and high permeability grain oriented, are used because the high permeability material presents a higher deterioration of it magnetic properties in the other direction than RD [13] compared to the conventional one. The evolution laws of R_μ and P_μ are shown in Fig. 3a and Fig. 3b. The best configuration is obtained for the static machine with the high permeability material, noted HGO35, which brings large reduction of core losses. This difference, up to 0.7 T, is mostly due to the magnetic properties from the linear part of the b(h) curve. Nevertheless, when $\hat{b}_{\mathrm{ag}}$ exceeded 0.7 T, the gain becomes modest in comparison to NO35 because the RD becomes saturated. It means that the magnetic field tends to go in the other directions. Despite this drawback, the static machine, made with high permeability GO material, offers less core losses compared to the other configurations.

III. Induction machine

A. Die-casting copper rotor

Magnetic materials endure a violent thermal shock during the die-casting process. In fact, this process involves heating the copper at a temperature of 1100 °C to 1200 °C. In order to determine the effect of this process on magnetic properties, a thermal shock, at 1100 °C, was applied to many Epstein frames. A standardized measurement system was used to determine the magnetic properties after this thermal treatment. Hence, the magnetic properties are minimally affected by this thermal shock. This result means that GO materials can be used with the die-casting copper squirrel cage. Nevertheless, due to realization constraints the lamination thickness has to be limited to 0.35 mm in order to prevent some damage on squirrel-cage and the stack.

B. No-load test

According to section III-A, the die casting copper process can be realized with GO electrical steel sheets. The original rotor, which is made with non oriented material and a die casting copper squirrel cage, is from an 11 kW four-pole induction machine. In order to make a comparison, the rotor with high permeability GO material is based on the same rotor design. Moreover, the stator of this induction machine is used to test the rotors. In order to confirm the benefits of used GO materials for the rotor of induction machine, the different experiments are based on the no-load test. Hence, the core losses, stator Joule losses and mechanical losses of both configurations can be deduced. In order to determine the no-load losses, a precision digital power meter was used. From these tests, the mechanical losses are close to 140 W for each configuration. The active power is presented in Fig.4a. It clearly shows that the induction machine with the new rotor has a lower consumption. The core losses and the difference on it are given in Figs. 4b and 4c respectively. Core losses was reduced around 35 %. This result implies a decrease in rotor core losses which is due to slotting effect [14] but it does not explain the gain of 35 %. During the manufacturing process, the air-gap length is slightly different between the prototype and the serial production. This difference is around to 3 % on the air-gap thickness. Hence, the air-gap induction is different. That implies a reduction of stator core losses and a higher current for the prototype. The difference in active power consumption is less important compared to the difference on the core losses, as shown Fig.4a. Nevertheless, the gain on the active power consumption is around 12 % at 230 V.

IV. Conclusion

In this paper, a new magnetic structure applied to the rotor with die casting copper squirrel cage has been investigated. The new magnetic structure was tested on a simple experiment in order to demonstrate the effective reduction of core losses. Replacing non oriented material by grain oriented material on rotor in the die casting copper process leads to a significant reduction of the core losses and active power consumption in the induction motor. In the extended paper, a finite element analysis of the static machine will be shown in order to explain the differences between the different structure. The measurements on Epstein frames will also be presented as well as the efficiency measurements.

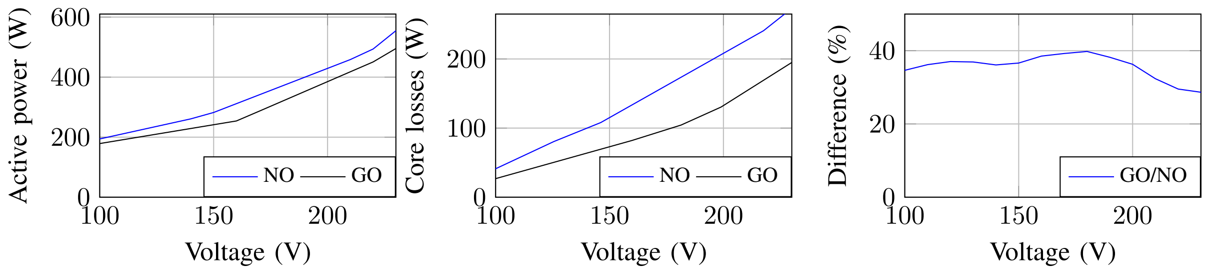

(a) (b) (c)

Fig. 4. (a) Active power consumption at different voltage levels. (b) Core losses at different voltage levels. (c) Difference of Core losses at different voltage levels;

Acknowledgment

This work was supported by FAVI, a French company specialized in copper alloy pressure die-casting. This program is also supported by ThyssenKrupp Electrical Steel which provided us the grain oriented materials.

References

[1] "Efficiency classes of line operated AC motors, IEC60034-30," 2014.

[2] A. Boglietti, A. Cavagnino, L. Ferraris, M. Lazzari, and G. Luparia, "No tooling cost process for induction motors energy efficiency improvements," *IEEE Transactions on Industry Applications*, vol. 41, no. 3, pp. 808–816, May 2005.

[3] L. Alberti, N. Bianchi, A. Boglietti, and A. Cavagnino, "Core axial lengthening as effective solution to improve the induction motor efficiency classes," *IEEE Trans. Ind. Appl.*, vol. 50, no. 1, pp. 218–225, 2014.

[4] E. B. Agamloh, A. Boglietti, and A. Cavagnino, "The incremental design efficiency improvement of commercially manufactured induction motors," *IEEE Transactions on Industry Applications*, vol. 49, no. 6, pp. 2496–2504, Nov 2013.

[5] J. L. Kirtley, J. G. Cowie, E. F. Brush, D. T. Peters, and R. Kimmich, "Improving induction motor efficiency with die-cast copper rotor cages," *2007 IEEE Power Eng. Soc. Gen. Meet. PES*, pp. 1–6, 2007.

[6] E. Chiricozzi, F. Parasiliti, and M. Villani, "New materials and innovative technologies to improve the efficiency of three-phase induction motors. a case study," in *16 th International Conference on Electrical Machines ICEM*, 2004, pp. 5–8.

[7] D. Ashwin, S. Ashok, M. Dixit, and V. Chavan, "Design optimization of 15 kW , 2-pole induction motor to achieve IE4 efficiency level with copper die casting," *Adv. Power Energy (TAP Energy), 2015 Int. Conf.*, pp. 98–102, 2015.

[8] S. Cical, L. Albini, F. Parasiliti, and M. Villani, "Design of a permanent magnet synchronous motor with grain oriented electrical steel for direct-drive elevators," in *2012 XXth International Conference on Electrical Machines*, Sept 2012, pp. 1256–1263.

[9] Y. Sugawara and K. Akatsu, "Characteristics of a switched reluctance motor using grain-oriented electric steel sheet," in *2013 IEEE ECCE Asia Downunder*, June 2013, pp. 1105–1110.

[10] S. Lopez, B. Cassoret, J. F. Brudny, L. Lefebvre, and J. N. Vincent, "Grain oriented steel assembly characterization for the development of high efficiency AC rotating electrical machines," *IEEE Trans. Magn.*, vol. 45, no. 10, pp. 4161–4164, 2009.

[11] B. Cassoret, S. Lopez, J.-F. Brudny, and T. Belgrand, "Non-Segmented Grain Oriented Steel in Induction Machines," *Progress In Electromagnetics Research C*, vol. 47, pp. 1–10, 2014.

[12] G. Parent, R. Penin, J. P. Lecointe, J. F. Brudny, and T. Belgrand, "Analysis of the magnetic flux distribution in a new shifted non-segmented grain oriented AC motor magnetic circuit," *IEEE Trans. Magn.*, vol. 49, no. 5, pp. 1977–1980, 2013.

[13] G. H. Shirkoohi and M. A. M. Arikat, "Anisotropic Properties of High Permeability Grain-oriented 3.25% Si-Fe Electrical Steel," *IEEE Trans. Magn.*, vol. 30, no. 2, pp. 928–930, 1994.

[14] J. Brudny and R. Romary, "Analysis of the slotting effect on the induction machine dynamic iron losses," *Computer Fields Models of Electromagnetic Devices*, vol. 34, pp. 27–73, 2010.